

## Discovery of Huperzine A–Tacrine Hybrids as Potent Inhibitors of Human Cholinesterases Targeting Their Midgorge Recognition Sites

Sandra Gemma,<sup>†,‡</sup> Emanuele Gabellieri,<sup>†,‡</sup> Paul Huleatt,<sup>†</sup> Caterina Fattorusso,<sup>‡,§</sup> Marianna Borriello,<sup>‡,§</sup> Bruno Catalanotti,<sup>‡,§</sup> Stefania Butini,<sup>†,‡</sup> Meri De Angelis,<sup>†,‡</sup> Ettore Novellino,<sup>‡,§</sup> Vito Nacci,<sup>†,‡</sup> Tatyana Belinskaya,<sup>||</sup> Ashima Saxena,<sup>||</sup> and Giuseppe Campiani<sup>\*,†,‡</sup>

Dipartimento Farmaco Chimico Tecnologico, Via Aldo Moro, and European Research Centre for Drug Discovery & Development, Università di Siena, 53100 Siena, Italy, Dipartimento di Chimica delle Sostanze Naturali and Dipartimento di Chimica Farmaceutica e Tossicologica, Università di Napoli Federico II, via D. Montesano 49, 80131 Napoli, Italy, and Division of Biochemistry, Walter Reed Army Institute of Research, Silver Spring, Maryland 20910

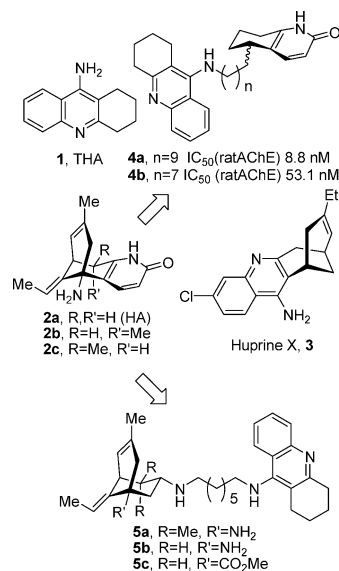
Received March 7, 2006

We describe herein the development of novel huperzine A–tacrine hybrids characterized by 3-methylbicyclo-[3.3.1]non-3-ene scaffolds. These compounds were specifically designed to establish tight interactions, through different binding modes, with the midgorge recognition sites of human acetylcholinesterase (hAChE: Y72, D74) and human butyrylcholinesterase (hBuChE: N68, D70) and their catalytic or peripheral sites. Compounds **5a–c** show a markedly improved biological profile relative to tacrine and huperzine A.

### Introduction

The human central nervous system (CNS) contains two different cholinesterases: acetylcholinesterase (hAChE) and butyrylcholinesterase (hBuChE). Although 50–60% homologous, these enzymes are encoded by different genes and clearly differ in substrate specificity and sensitivity to inhibitors, likely due mainly to structural differences in the active site gorge of the two enzymes, leading to a lower electrostatic gradient and a larger void in BuChE.<sup>1,2</sup> While AChE inhibitors (AChEIs) represent a well-established class of drugs for the symptomatic treatment of Alzheimer's disease (AD),<sup>3</sup> recent findings point to BuChE inhibition as an additional tool to increase the cholinergic activity in AD patients affected by severe symptoms.<sup>4</sup> Although the forebrain cholinergic system is clearly perturbed during mild to moderate AD, by the time the disease has progressed to its severe stage, AChE and choline acetyltransferase levels are as much as 85–90% lower than normal. Interestingly, it has been reported by several authors that this loss of AChE is accompanied by an increase in glial BuChE levels by up to 2-fold,<sup>3</sup> suggesting that BuChE can partly compensate for AChE action in severe AD.<sup>3–5</sup> Despite this topic still being a matter of debate,<sup>6</sup> clinical studies using rivastigmine, a potent inhibitor of both BuChE and AChE, proved the increased therapeutic efficacy of this compound in mild-to-moderate and moderately severe AD compared to currently used AChE selective inhibitors, indicating that clinical benefits of rivastigmine are related to its dual inhibitory action.<sup>7</sup> Four AChEIs have been approved by the European and US regulatory authorities: tacrine (THA, **1**, Chart 1), donepezil, rivastigmine, and galantamine. These drugs are often associated with adverse events (e.g., liver damage, nausea, and vomiting) and their therapeutic potential is limited. Huperzine A (HA, **2a**) is an alkaloid, presently under clinical evaluation.<sup>8</sup> As with the previously mentioned AChEIs, huperzine A interacts with the

Chart 1. Reference and Title Compounds



catalytic binding site of AChE, which is located at the bottom of a deep gorge. A second binding site, at the lip of the gorge, namely the peripheral “anionic” site (PAS), is located around 18 Å away from the active site.<sup>9</sup> Through the development of specific tacrine heterodimers, our group recently targeted a “midgorge recognition site” in hAChE. In addition, we uncovered the existence of a peripheral binding site and a midgorge interaction site also in the BuChE family of enzymes.<sup>10,11</sup> In the past, we have reported the synthesis of HA and of a large number of closely related analogues.<sup>12</sup> Others hybridized the structure of HA to synthesize huprine X (**3**),<sup>13</sup> a potent AChEI, which incorporates key structural features from both HA and THA. In addition, HA–THA hybrids (**4a** and **4b**) containing the bicyclic tetrahydroquinolinone fragment of HA have been reported.<sup>14</sup> Huprine X interacts with the catalytic site of AChE, displaying a low affinity for BuChE, while the hybrids described by Carrier can interact with the catalytic site and/or PAS of AChE, depending on the length of the linker. In particular, **4b** showed low affinity while its superior homologue **4a** (characterized by a 10-carbon methylene linker) displayed nanomolar

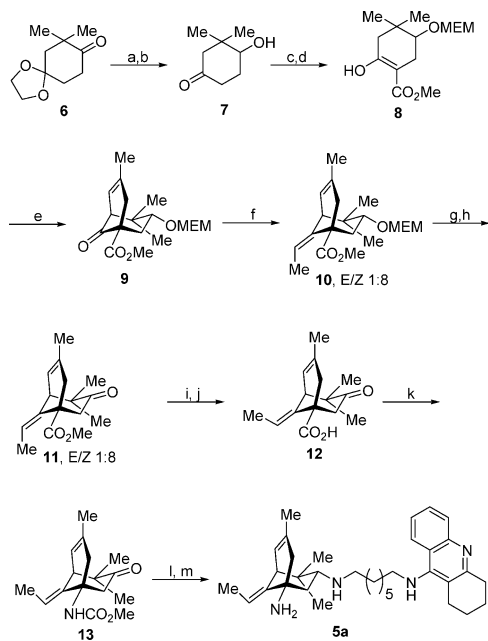
\* To whom correspondence should be addressed. Tel: 0039-0577-234172. Fax: 0039-0577-234333. E-mail: campiani@unisi.it.

<sup>†</sup> Dipartimento Farmaco Chimico Tecnologico, Università degli Studi di Siena.

<sup>‡</sup> European Research Centre for Drug Discovery and Development, Università di Siena.

<sup>§</sup> Università degli Studi di Napoli “Federico II”.

<sup>||</sup> Walter Reed Army Institute of Research.

Scheme 1<sup>a</sup>

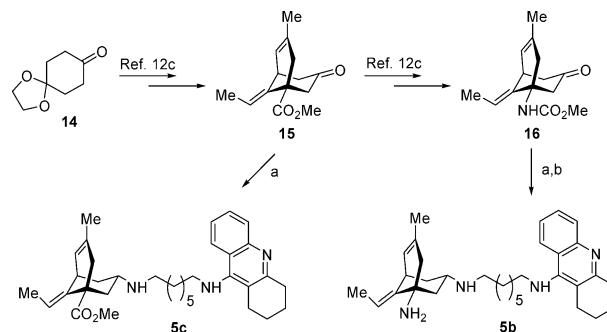
<sup>a</sup> Conditions: (a) NaBH<sub>4</sub>; (b) 1 N HCl; (c) MEMCl, DIPEA; (d) KH, 35% in mineral oil, DMC; (e) (1) methacrolein, TMG; (2) MsCl, Et<sub>3</sub>N, DMAP; (3) 2,4,6-collidine; (f) Ph<sub>3</sub>PtEtBr, KHMDS (0.5 M in toluene); (g) 1 N HCl; (h) PDC; (i) PhSH, AIBN; (j) NaOH 20%, MeOH/THF 1:2; (k) (1) (PhO)<sub>2</sub>PON<sub>3</sub>, Et<sub>3</sub>N; (2) MeOH, reflux; (l) (1) *N*-(7-aminoheptyl)-1,2,3,4-tetrahydroacridin-9-amine, Ti(*O*-*i*-Pr)<sub>4</sub>; (2) NaBH<sub>3</sub>CN; (m) (1) Me<sub>3</sub>SiI; (2) MeOH, reflux.

affinity, likely due to the interaction of the second protonatable nitrogen with rat AChE PAS.<sup>14</sup> Interestingly, **4a** and **4b** were found to be poorly active on rat BuChE.<sup>14</sup> Since much evidence suggests that BuChE may represent an intriguing target for the treatment of AD,<sup>1–4,7,8</sup> enzyme selectivity may not be a key issue in drug development for treating neurodegenerative disorders of the Alzheimer's type, and specific ligands targeting both enzymes may represent a new and valuable therapeutic approach for use in mild, moderate, and severe dementia. Accordingly, taking into account the information previously acquired on the existence of multiple interaction sites in either the AChE or the BuChE family of enzymes (catalytic, midgorge, and peripheral), we developed the new HA–THA hybrids **5a–c**, shown in Chart 1, with the aim to obtain inhibitors targeting both enzymes. These compounds are characterized by a nanomolar inhibitory activity on both hAChE and hBuChE.

## Chemistry

Our background in the synthesis of potent structural analogues of HA (a methyl group at C-10 axial and equatorial positions provided analogues more potent than HA)<sup>12b</sup> was exploited. For the synthesis of compound **5a**, our main goal was the setup of a suitable synthetic strategy to obtain the (±)-methyl (9*E*)-9-ethylidene-3,6,6-trimethyl-7-oxobicyclo[3.3.1]non-3-en-1-ylcarbamate key intermediate **13**.

The synthesis begins by reducing the carbonyl group of the known monoethylene ketal **6**<sup>15</sup> (Scheme 1) using sodium borohydride followed by deprotection of the ketal function by exposure to 1 N hydrochloric acid in acetone to obtain ketol **7**. The hydroxy group was then protected as a methoxyethoxymethyl ether (MEM ether). The resulting compound was regioselectively transformed into the β-keto ester **8** by means of potassium hydride and dimethyl carbonate (DMC). This reaction, carried out using Mander's reagent,<sup>16</sup> failed. The introduction of the unsaturated carbon bridge across the β-keto

Scheme 2<sup>a</sup>

<sup>a</sup> Conditions: (a) (1) *N*-(7-aminoheptyl)-1,2,3,4-tetrahydroacridin-9-amine, AcOH, pH 6; (2) NaBH<sub>3</sub>CN; (b) (1) Me<sub>3</sub>SiI; (2) MeOH, reflux.

ester **8** was achieved by a Michael addition–aldol reaction sequence catalyzed by 1,1,3,3-tetramethylguanidine (TMG) to yield a bicyclic ketol intermediate.<sup>12c</sup> The *endo*-olefin **9** was finally obtained by dehydration of the alcohol precursor (as a mixture of stereoisomers) through a two-step process involving mesylate formation followed by collidine-induced elimination. Starting from β-keto ester **9** the next step of the synthetic plan required the installation of the (*E*)-ethylidene side chain at C9. A standard Wittig olefination protocol employing *n*-BuLi and ethyl(triphenylphosphonium)bromide furnished only trace amount of the desired olefination product along with a complex mixture of fragmentation products of the bridged bicyclic skeleton and of the MEM ether. Investigation of a variety of reaction conditions led us to obtain a 8:1 mixture of (*Z*)- and (*E*)-alkenes **10** in 75% yield when potassium bis(trimethylsilyl)amide and ethyl(triphenylphosphonium)bromide were used.<sup>17</sup> As the reaction product consisted largely of the incorrect isomer, mixture **10** was subjected to an isomerization reaction employing thiophenol and 2,2'-azobisisobutyronitrile (AIBN), which resulted in an intractable mixture, probably due to the instability of MEM ether under radical conditions. Alternatively, hydrochloric acid-promoted deprotection of the hydroxy group followed by oxidation of the alcohol using PDC furnished ketone **11** in good overall yield. Radical isomerization of the (*Z*)-ethylidene chain of the resulting ketone **11** afforded an 18:1 mixture of (*E*)- and (*Z*)-olefins in 95% yield. Next, the ester was hydrolyzed by 20% sodium hydroxide in a 2:1 tetrahydrofuran/methanol mixture to furnish the *E*-acid **12** as a single geometric isomer (the more hindered *Z*-isomer failed to undergo hydrolysis under these conditions). The resulting acid was treated with diphenyl azidophosphate, and the intermediate isocyanate was reacted with methanol to provide the key urethane intermediate **13**. Initial attempts to carry out the reductive amination reaction of ketone **13** with *N*-(7-aminoheptyl)-1,2,3,4-tetrahydroacridin-9-amine<sup>18</sup> proved to be problematic. A variety of reaction conditions, using different dehydrating agents, solvents, and reaction conditions (temperature, sealed tube reactions) failed to afford the desired compound or the corresponding imine intermediate. Success was ultimately achieved through a two-step protocol that involved carbonyl activation by titanium tetraisopropoxide followed by treatment of the crude reaction mixture with sodium cyanoborohydride in ethanol.<sup>19</sup> Trimethylsilyl iodide-promoted deprotection of the carbamate group finally furnished the desired heterodimer **5a**.

The synthesis of compounds **5b** and **5c** is described in Scheme 2. Ketones **15** and **16**, readily accessible from commercially available 1,4-cyclohexanedione monoethylene ketal following a previously described procedure,<sup>12c</sup> were reacted with *N*-(7-

aminoheptyl)-1,2,3,4-tetrahydroacridin-9-amine to furnish final compounds **5c** and, after carbamate deprotection, **5b**.

## Results and Discussion

We previously reported<sup>10,11</sup> that a protonatable nitrogen at the tether level of tacrine homo- and heterodimers was a key determinant for potency improvement toward ChEs. This is due to interactions with the midgorge recognition site, characterized by the presence of a conserved Asp residue (hAChE, D74; hBuChE, D70). Interestingly, at the midgorge level AChE and BuChE differ in their amino acid composition, since AChEs present several aromatic residues that are replaced by aliphatic ones in BuChEs. These structural differences are responsible for the larger electrostatic gradient and for the narrower void along the AChE gorge with respect to BuChE, affecting ligand selectivity.<sup>10,11</sup> Flexible docking studies showed that **5a–c** can adopt different binding modes within hAChE and hBuChE active site gorges, and results are displayed in Figures 1 and 2. The stronger electrostatic gradient present along the AChE gorge drives the diprotonated (see Table 1 of the Supporting Information) 3-methylbicyclo[3.3.1]non-3-ene moiety of **5b** ( $K_{ihAChE} = 15.7$  nM) in the catalytic site. At this level the protonated primary amine group of **5b** interacts with W86, through a cation– $\pi$  interaction, and H447 and G448, through a bridged water molecule, placing the bridged 3-methyl group and the ethylidene chain in a similar orientation to HA in complex with TcAChE (PDB code 1VOT). In addition, the secondary protonated amine of the bicyclic scaffold interacts with D74 and presents a suitable H-bond distance from the Y124 side chain oxygen (2.8 Å), also establishing a water-mediated hydrogen bond with T83. Finally, the THA moiety protrudes to the PAS, setting up a polarized  $\pi$ – $\pi$  interaction with W286 (Figure 1A). On the other hand, the introduction of two methyl substituents at C-4 (**5a**;  $K_{ihAChE} = 16.5$  nM) induces a partial rotation of the HA moiety, which results in a direct interaction between the **5a** primary amine group and the catalytic site (G448, H447) and in the displacement of the water molecule present in **5b** (Figure 1, A vs B). Compound **5a** preserves a direct interaction with D74 through the secondary amino group, but its orientation promotes an H-bond with the Y337 side chain (Y124 in **5b**). The results of our docking studies suggested an opposite binding mode for **5a** and **5b** in hBuChE, with respect to hAChE. This also reflects the different activities of THA and HA toward both enzymes (Table 1). Indeed, **5a** and **5b** place the THA and the 3-methylbicyclo[3.3.1]non-3-ene moieties in the BuChE catalytic and midgorge sites, respectively (Figure 2A,B). In particular, the bulkier C-4 methyl groups of **5a** ( $K_{ihBuChE} = 20.8$  nM; Figure 2B) are perfectly accommodated in the lipophilic environment at the midgorge level of the enzyme: (i) establishing favorable van der Waals interactions with P285 and I69, (ii) directly anchoring the protonated primary amine group to D70 and to the side chain carbonyl oxygen of N68, and (iii) interacting with D70 (secondary amine group) and Q71 (primary amine group) through a water-mediated hydrogen-bond network. This accommodation allows an optimal orientation of the THA moiety in the catalytic site (Figure 2B). A similar orientation is observed for compound **5c** ( $K_{ihBuChE} = 19.5$  nM), thus allowing an optimal  $\pi$ – $\pi$  interaction between W82 and the THA moiety and also H-bond formation between the exo-cyclic THA nitrogen and T120 side chain (Figure 2C). On the contrary, for the less hindered compound **5b** ( $K_{ihBuChE} = 30.8$  nM) the electrostatic interaction with D70 prevails, constraining **5b** in an orientation that weakens interactions with the catalytic site (Figure 2A). As we have previously observed,<sup>10,11</sup> the potency of multisite inhibitors (i.e., binding more than one site along

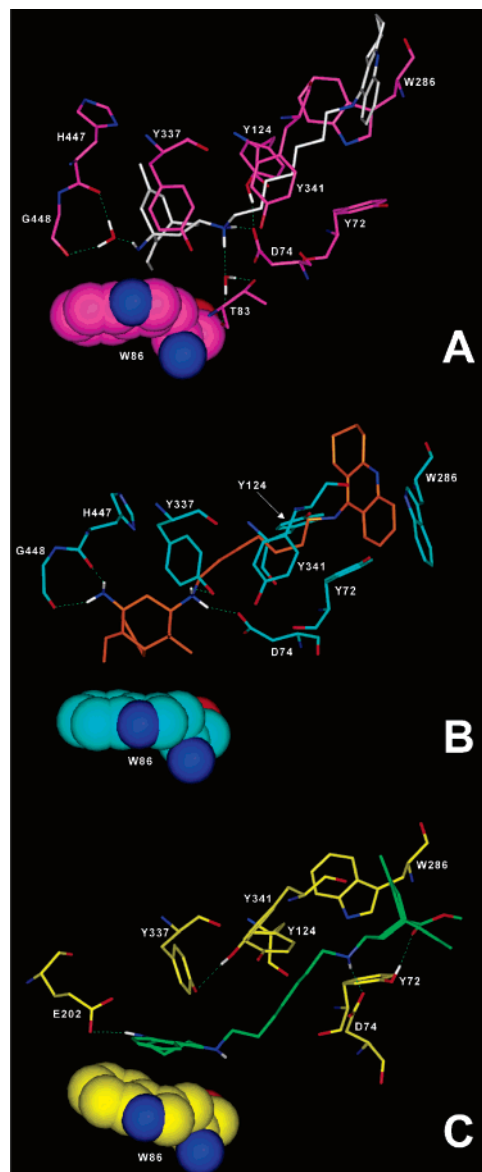


**Figure 1.** Docked complexes of (A) **5b**/hAChE (ligand, white; protein, magenta), (B) **5a**/hAChE (ligand, orange; protein, cyan), and (C) **5c**/hAChE (ligand, green; protein, yellow). Heteroatoms and water molecules are colored by atom type. The van der Waals volume of W86 is displayed. Hydrogen bonds are highlighted by green dashed lines. Ligand and protein hydrogens are omitted for clarity, with the exception of those involved in hydrogen-bond interactions.

the active site gorge of ChEs) is modulated by the mutual orientation of the binding groups of the ligand.

Compound **5c** contains an ester function in place of the primary amine group on the HA fragment. Consequently, this substitution induces a change in the binding mode of **5c** ( $K_{ihAChE} = 6.4$  nM) to AChE with respect to **5a,b**, placing the THA moiety in the catalytic site similar to that observed in BuChE with the HA fragment favorably interacting with W286 (PAS) (Figure 1C). Moreover, **5c** preserves the electrostatic interaction at the midgorge level with D74 and establishes an additional interaction with Y72 (Figure 1C). An H-bond is formed between the hydroxyl group of the Y72 side chain and the carbonyl oxygen of the inhibitor. Interestingly, **5c** establishes an analogous H-bond interaction with the side chain of the corresponding residue in hBuChE (N68; Figure 2C). The introduction of the 3-methylbicyclo[3.3.1]non-3-ene scaffold in THA–HA hybrids conferred a significant increase in inhibitory potency on AChE

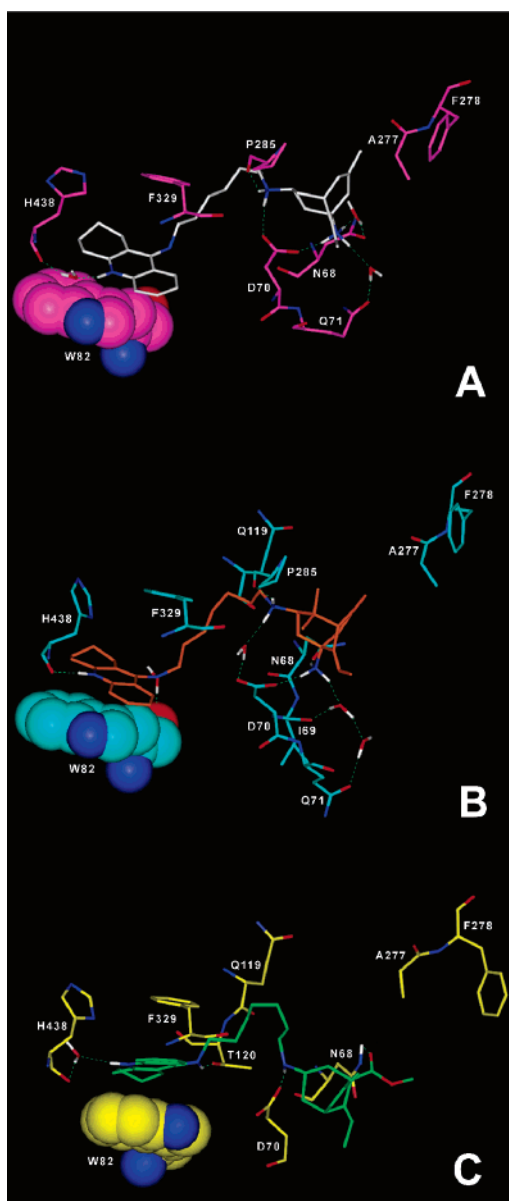


**Figure 2.** Docked complexes of (A) **5b**/hBuChE (ligand, white; protein, magenta), (B) **5a**/hBuChE (ligand, orange; protein, cyan), and (C) **5c**/hBuChE (ligand, green; protein, yellow). Heteroatoms and water molecules are colored by atom type. The van der Waals volume of W86 is displayed. Hydrogen bonds are highlighted by green dashed lines. Ligand and protein hydrogens are omitted for clarity, with the exception of those involved in hydrogen-bond interactions.

**Table 1.** Dissociation Constants for the Inhibition of hAChE and hBuChE by Compounds **5a–c**

compd	$K_i$ (nM) (SD) <sup>a</sup>	
	hAChE	hBuChE
<b>5a</b>	16.5 ± 0.3	20.8 ± 2.6
<b>5b</b>	15.7 ± 0.9	30.8 ± 2.0
<b>5c</b>	6.4 ± 0.8	19.5 ± 1.9
THA ( <b>1</b> )	137.0	7.0
(±)-HA ( <b>2a</b> )	47.0	> 1000
huprine X ( <b>3</b> ) <sup>b</sup>	0.026	120

<sup>a</sup>  $K_i$  is the mean of at least three determinations. <sup>b</sup> Reference 13.

with respect to **4b**. In addition, a significant potency against BuChE was also observed.

## Conclusions

In summary, we designed and synthesized novel and potent HA/THA hybrids targeting the midgorge recognition site of both

hAChE and hBuChE. In particular, in hBuChE we hypothesized a binding mode involving interactions at the catalytic site (W82 and H438) and at the recently discovered midgorge recognition site (D70, N68, and Q71). On the other hand, by adopting an “upside down” binding-mode on hAChE, compounds **5a** and **5b** showed interactions with the catalytic and the midgorge and the PAS (W286) recognition sites. Conversely, the potent inhibitor **5c** places the THA moiety in the catalytic site, still being able to interact with the three AChE binding sites and establishing an extra interaction with Y72 through the carbonyl oxygen of its ester group. Compounds **5a–c** represent potent ChE multisite inhibitors of human ChEs, showing comparable inhibitory activities for both hAChE and hBuChE, thus providing useful tools for the evaluation of a new therapeutic approach against the cognitive impairment in moderate and severe AD.

## Experimental Section

**(9E)-N1-(7-(1,2,3,4-Tetrahydroacridin-9-ylamino)heptyl)-9-ethylidene-4,4,7-trimethylbicyclo[3.3.1]non-6-ene-1,3-diamine (5a).** A mixture of **13** (30.0 mg, 0.108 mmol), *N*-(7-aminoheptyl)-1,2,3,4-tetrahydroacridin-9-amine<sup>18</sup> (118.4 mg, 0.46 mmol), and titanium tetraisopropoxide (1.48 mmol, 0.4 mL) was stirred at room temperature for 48 h. Then NaBH<sub>3</sub>CN (44.0 mg, 0.70 mmol) and ethanol (2.0 mL) were added, and stirring was continued for 120 h. Water was added, and the solid was removed by vacuum filtration through a bed of silica gel, which was subsequently washed with ethanol. The filtered solution was concentrated and excess NaBH<sub>3</sub>CN was destroyed by addition of aqueous hydrochloric acid and stirring for 1 h. The mixture was made alkaline with 1 N aqueous sodium hydroxide and extracted with dichloromethane. The organic extracts were dried (Na<sub>2</sub>SO<sub>4</sub>), and the solvent was removed. The residue was purified by flash chromatography eluting with a 10:1:0.5 mixture of EtOAc, MeOH, and triethylamine to afford a carbamate intermediate (16.7 mg, 30%) as colorless oil: <sup>1</sup>H NMR (CDCl<sub>3</sub>) δ 7.98–7.96 (m, 2H), 7.58–7.54 (m, 1H), 7.37–7.33 (m, 1H), 5.42 (d, *J* = 5.4 Hz, 1H), 5.22 (q, *J* = 6.6 Hz, 1H), 4.77 (bs, 1H), 3.63 (s, 3H), 3.53 (t, *J* = 6.8 Hz, 2H), 3.11–3.09 (m, 2H), 2.88 (d, *J* = 5.4 Hz, 1H), 2.73–2.63 (m, 5H), 2.57 (dd, *J* = 4.8, 12.0 Hz, 1H), 2.49 (d, *J* = 8.5 Hz, 1H), 2.44–2.34 (m, 1H), 2.25–2.19 (m, 1H), 1.95–1.91 (m, 4H), 1.64–1.57 (m, 6H), 1.38–1.18 (m, 10H), 0.91 (s, 3H), 0.86 (s, 3H); ES/MS *m/z* 573 (M<sup>+</sup> + H). To a solution of the above compound (10 mg, 0.019 mmol) in dry chloroform (0.5 mL) was added iodotrimethylsilane (15.6 μL, 0.11 mmol), and the resulting mixture was heated under reflux for 5 h. After cooling to room temperature, the solvent was removed in vacuo, the residue was dissolved in dry methanol (1 mL), and the solution was heated under reflux. After 18 h, the solvent was removed and the residue was purified by flash chromatography eluting with a 20:1:1 mixture of ethyl acetate, methanol, and ammonium hydroxide (30%) to obtain 1.1 mg (12%) of **5a** as a colorless oil: <sup>1</sup>H NMR (CDCl<sub>3</sub> + D<sub>2</sub>O) δ 7.96–7.91 (m, 2H), 7.56–7.52 (m, 1H), 7.35–7.31 (m, 1H), 5.43–5.38 (m, 2H), 3.48 (t, *J* = 7.2 Hz, 2H), 3.07–3.06 (m, 2H), 2.88 (d, *J* = 6.2 Hz, 1H), 2.70–2.66 (m, 5H), 2.57 (dd, *J* = 4.9, 12.0 Hz, 1H), 2.44–2.38 (m, 2H), 2.19–2.14 (m, 1H), 1.98–1.90 (m, 4H), 1.67–1.59 (m, 6H), 1.47–1.24 (m, 10H), 0.96 (s, 3H), 0.76 (s, 3H); ESI-MS *m/z* 515 (M + H)<sup>+</sup>. Anal. (C<sub>34</sub>H<sub>50</sub>N<sub>4</sub>) C, H, N.

**(9E)-N1-(7-(1,2,3,4-Tetrahydroacridin-9-ylamino)heptyl)-9-ethylidene-7-methylbicyclo[3.3.1]non-6-ene-1,3-diamine (5b).** To a solution of *N*-(7-aminoheptyl)-1,2,3,4-tetrahydroacridin-9-amine<sup>18</sup> (49.0 mg, 0.16 mmol) in dry tetrahydrofuran and methanol (1:1, 2 mL), maintained at pH 6 by addition of glacial acetic acid, was added **16** (18.0 mg, 0.07 mmol). The mixture was stirred at room temperature for 1 h and then NaBH<sub>3</sub>CN (22.0 mg, 0.36 mmol) was added, and the reaction mixture was heated to 50 °C. After 72 h the reaction mixture was cooled to room temperature, water was added, the solvent was removed in vacuo, and the aqueous phase was extracted with chloroform. The organic extracts were dried (Na<sub>2</sub>SO<sub>4</sub>) and the solvent was removed. The residue was purified

by flash chromatography eluting with a 20:1:1 mixture of ethyl acetate, methanol, and ammonium hydroxide (30%) to afford 10.0 mg (26%) of a carbamate intermediate as a colorless oil: ESI-MS  $m/z$  545 [M + H]<sup>+</sup>, 513 (100), 470, 338, 312, 295, 199. To a solution of the above carbamate (10 mg, 0.018 mmol) in dry chloroform (0.5 mL) was added iodotrimethylsilane (15.6  $\mu$ L, 0.11 mmol), and the resulting mixture was heated under reflux for 5 h. After cooling to room temperature, the solvent was removed in vacuo, the residue was dissolved in dry methanol (1 mL) and the solution was heated under reflux. After 18 h the solvent was removed and the residue was purified by flash chromatography eluting with a 20:1:1 mixture of ethyl acetate, methanol, and ammonium hydroxide (30%) to obtain 1.1 mg (12%) of **5b** as a colorless oil: <sup>1</sup>H NMR (CDCl<sub>3</sub> + D<sub>2</sub>O)  $\delta$  7.93–7.91 (m, 2H), 7.55–7.53 (m, 1H), 7.30–7.27 (m, 1H), 5.36–5.28 (m, 2H), 3.68–3.60 (m, 3H), 3.51 (t,  $J$  = 8.0 Hz, 2H), 3.15–2.87 (m, 3H), 2.75–2.51 (m, 6H), 2.31–2.22 (m, 2H), 2.03–1.75 (m, 4H), 1.60–1.52 (m, 6H), 1.51–1.22 (m, 10H); ESI-MS  $m/z$  487 (M + H)<sup>+</sup>. Anal. (C<sub>32</sub>H<sub>46</sub>N<sub>4</sub>) C, H, N.

(9E)-7-(7-(1,2,3,4-Tetrahydroacridin-9-ylamino)heptylamino)-9-ethylidene-3-methylbicyclo[3.3.1]non-3-ene-1-carboxylic Acid Methyl Ester (**5c**). Reductive amination of ketone **15** and *N*-(7-aminoheptyl)-1,2,3,4-tetrahydroacridin-9-amine<sup>18</sup> was performed as described for the synthesis of **5b** to afford the title compound **5c** in 23% yield as a colorless oil: <sup>1</sup>H NMR (CDCl<sub>3</sub> + D<sub>2</sub>O)  $\delta$  7.96–7.89 (m, 2H), 7.57–7.50 (m, 1H), 7.37–7.29 (m, 1H), 5.47–5.37 (m, 1H), 4.91–4.87 (m, 1H), 3.73 (s, 3H), 3.47 (t,  $J$  = 6.9 Hz, 2H), 3.28–3.15 (m, 3H), 3.05–2.97 (m, 2H), 2.77–2.55 (m, 4H), 2.50–2.47 (m, 3H), 2.34–2.20 (m, 2H), 1.97–1.90 (m, 4H), 1.65–1.57 (m, 6H), 1.41–1.21 (m, 10H); ESI-MS  $m/z$  530 (M + H)<sup>+</sup>. Anal. (C<sub>34</sub>H<sub>47</sub>N<sub>3</sub>O<sub>2</sub>) C, H, N.

**Acknowledgment.** Authors thank MIUR (Roma) for financial support. The opinions or assertions contained herein are the private views of the authors and are not to be construed as official or as reflecting the views of the United States Army or Department of Defense.

**Supporting Information Available:** Experimental details for **13** and molecular modeling and pharmacology for **5a–c**. This material is available free of charge via the Internet at <http://pubs.acs.org>.

## References

- Gentry, M. K.; Doctor, B. P. In *Cholinesterases: Structure, function, mechanism, genetics, and cell biology*; Massoulie, J., Bacou, F., Barnard, E. A., Chatonnet, A., Doctor, B. P., Eds.; American Chemical Society: Washington, DC, 1991; pp 394–398.
- Saxena, A.; Redman, A. M. G.; Jiang, X.; Lockridge, O.; Doctor, B. P. Differences in active site gorge dimension of cholinesterases revealed by binding of inhibitors to human butyrylcholinesterase. *Biochemistry* **1997**, *36*, 14642–14651.
- Giacobini, E. Cholinergic functions in Alzheimer's disease. *Int. J. Geriatr. Psychiatry* **2003**, *18*, S1–S5, and references therein.
- Greig, N. H.; Utsuki, T.; Yu, Q.-S.; Zhu, X.; Holloway, H. W.; Perry, T.; Lee, B.; Ingram, D. K.; Lahiri, D. K. A new therapeutic target in Alzheimer's disease treatment: Attention to butyrylcholinesterase. *Curr. Med. Res. Opin.* **2001**, *17*, 1–6.
- Mesulam, M. M.; Guillozet, A.; Shaw, P.; Levey, A.; Duysen, E. G.; Lockridge, O. Acetylcholinesterase knockouts establish central cholinergic pathways and can use butyrylcholinesterase to hydrolyse acetylcholine. *Neuroscience* **2002**, *110*, 627–639.
- Kuhl, D. E.; Koeppe, R. A.; Snyder, S. E.; Minoshima, S.; Frey, K. A.; Kilbourn, M. R. In vivo butyrylcholinesterase activity is not increased in Alzheimer's disease synapses. *Ann. Neurol.* **2006**, *59*, 13–20.
- (a) Lane, R. M.; Potkin, S. G.; Enz, A. Targeting acetylcholinesterase and butyrylcholinesterase in dementia. *Int. J. Neuropsychopharmacol.* **2006**, *1*, 101–124. (b) Bartorelli, L.; Giraldo, C.; Saccardo, M.; Cammarata, S.; Bottini, G.; Fasanaro, A. M.; Trequattrini, A. Effects of switching from an AChE inhibitor to a dual AChE–BuChE inhibitor in patients with Alzheimer's disease. *Curr. Med. Res. Opin.* **2005**, *11*, 1809–1818.
- Jiang, H.; Luo, X.; Bai, D. Progress in clinical, pharmacological, chemical and structural biological studies of huperzine A: A drug of traditional Chinese medicine origin for the treatment of Alzheimer's disease. *Curr. Med. Chem.* **2003**, *10*, 2231–2252.
- Pang, Y.-P.; Quiram, P.; Jelacic, T.; Hong, F. Highly potent, selective, and low cost bis-tetrahydroaminacrine inhibitors of acetylcholinesterase. Steps toward novel drugs for treating Alzheimer's disease. *J. Biol. Chem.* **1996**, *271*, 23646–23649.
- Savini, L.; Gaeta, L.; Fattorusso, C.; Catalanotti, B.; Campiani, G.; Chiasserini, L.; Pellerano, C.; Novellino, E.; McKissic, D.; Saxena, A. Specific targeting of acetylcholinesterase and butyrylcholinesterase recognition sites. Rational design of novel, selective, and highly potent cholinesterase inhibitors. *J. Med. Chem.* **2003**, *46*, 1–4.
- Campiani, G.; Fattorusso, C.; Butini, S.; Gaeta, A.; Agnusdei, M.; Gemma, S.; Persico, P.; Catalanotti, B.; Savini, L.; Nacci, V.; Novellino, E.; Holloway, W.; Greig, N. H.; Belinskaya, T.; Fedorko, J. M.; Saxena, A. Development of molecular probes for the identification of extra interaction sites in the mid-gorge and peripheral sites of butyrylcholinesterase (BuChE). Rational design of novel, selective, and highly potent BuChE inhibitors. *J. Med. Chem.* **2005**, *48*, 1919–1929.
- (a) Campiani, G.; Sun, L. Q.; Kozikowski, A. P.; Aagaard, P.; McKinney, M. A palladium-catalyzed route to huperzine A and its analogues and their anticholinesterase activity. *J. Org. Chem.* **1993**, *58*, 7660–7669. (b) Kozikowski, A. P.; Campiani, G.; Sun, L.-Q.; Wang, S.; Saxena, A.; Doctor, B. P. Identification of a more potent analogue of the naturally occurring alkaloid huperzine A. Predictive molecular modeling of its interaction with AChE. *J. Am. Chem. Soc.* **1996**, *118*, 11357–11362. (c) Kozikowski, A. P.; Campiani, G.; Tückmantel, W. An approach to open chain modified heterocyclic analogues of the acetylcholinesterase inhibitor, Huperzine A, through a bicyclo[3.3.1]nonane intermediate. *Heterocycles* **1994**, *39*, 101–116. (d) Gemma, S.; Butini, S.; Fattorusso, C.; Fiorini, I.; Nacci, V.; McKissic, D.; Saxena, A.; Campiani, G. A palladium-catalyzed synthetic approach to new huperzine A analogues modified at the pyridone ring. *Tetrahedron* **2003**, *59*, 87–93.
- Camps, P.; Cusack, B.; Mallender, W. D.; El Achab, R.; Morral, J.; Munoz, D. T.; Rosenberry, T. L. Huprine X is a novel high-affinity inhibitor of acetylcholinesterase that is of interest for treatment of Alzheimer's disease. *Mol. Pharmacol.* **2000**, *57*, 409–417.
- Carlier, P. R.; Du, D.-M.; Han, Y.; Liu, J.; Pang, Y.-P. Potent, easily synthesized huperzine A–tacrine hybrid acetylcholinesterase inhibitors. *Bioorg. Med. Chem. Lett.* **1999**, *9*, 2335–2338.
- Nelson, L. A. K.; Shaw, A. C.; Abrams, S. R. Synthesis of (+)-, (–)-, and (±)-7'-hydroxyabscisic acid. *Tetrahedron* **1991**, *47*, 3259–3270.
- Mander, L. N.; Sethi, S. P. Regioselective synthesis of  $\beta$ -ketoesters from lithium enolates and methyl cyanofornate. *Tetrahedron Lett.* **1983**, 5425–5428.
- Sreekumar, C.; Darst, K. P.; Still, W. C. A direct synthesis of Z-trisubstituted allylic alcohols via the Wittig reaction. *J. Org. Chem.* **1980**, *45*, 4260–4262.
- Carlier, P. R.; Chow, E. S.-H.; Han, Y.; Liu, J.; Yazal, J.; Pang, Y.-P. Heterodimeric tacrine-based acetylcholinesterase inhibitors: Investigating ligand–peripheral site interactions. *J. Med. Chem.* **1999**, *42*, 4225–4231.
- Wagermann, R.; Vilsmaier, E.; Maas, G. Spatially fixed oligoamines IV. 1 flexibility and protonation of meander-type octamines. *Tetrahedron* **1995**, 8815–8826.

JM060257T